MOEM

Modern Electronic Materials 4(1): 1–5
DOI 10.3897/j.moem.4.1.33270

Research Article

# Thermally stimulated oxygen desorption in $Sr_2FeMoO_{6-\delta}$

Nikolay A. Kalanda[1]

1 *Scientific-Practical Materials Research Centre of NAS of Belarus, 220072, Belarus, Minsk, 19 P. Brovki Str., Belarus*

Corresponding author: *Nikolay A. Kalanda* (kalanda@physics.by)

**Received** 14 March 2018 ♦ **Accepted** 30 March 2018 ♦ **Published** 1 May 2018

**Citation:** Kalanda NA (2018) Thermally stimulated oxygen desorption in $Sr_2FeMoO_{6-\delta}$. Modern Electronic Materials 4(1): 1–5. https://doi.org/10.3897/j.moem.4.1.33270

## Abstract

Polycrystalline $Sr_2FeMoO_{6-\delta}$ specimens have been obtained by solid state synthesis from partially reduced $SrFeO_{2,52}$ and $SrMoO_4$ precursors. It has been shown that during oxygen desorption from the $Sr_2FeMoO_{6-\delta}$ compound in polythermal mode in a 5%$H_2$/Ar gas flow at different heating rates, the oxygen index 6-δ depends on the heating rate and does not achieve saturation at $T$ = 1420 K. Oxygen diffusion activation energy calculation using the Merzhanov method has shown that at an early stage of oxygen desorption from the $Sr_2FeMoO_{6-\delta}$ compound the oxygen diffusion activation energy is the lowest $E_a$ = 76.7 kJ/mole at δ = 0.005. With an increase in the concentration of oxygen vacancies, the oxygen diffusion activation energy grows to $E_a$ = 156.3 kJ/mole at δ = 0.06. It has been found that the $d\delta/dt = f(T)$ and $d\delta/dt = f(\delta)$ functions have a typical break which allows one to divide oxygen desorption in two process stages. It is hypothesized that an increase in the concentration of oxygen vacancies $V_o^{\cdot\cdot}$ leads to their mutual interaction followed by ordering in the Fe/Mo-01 crystallographic planes with the formation of various types of associations.

## Keywords

strontium ferromolybdate, oxygen nonstoichiometry, defect formation, oxygen desorption

## 1. Introduction

The $Sr_2FeMoO_{6-\delta}$ double perovskite is a half-metal with a Curie temperature of 410–450 K characterized by high magnetoresistance (~3–10 %) in weak magnetic fields at room temperature [1–3]. This makes it quite promising for magnetic field sensors. Furthermore, strontium ferromolybdate with combined oxygen ionic and electronic conductivity is of great practical interest since it can be used for the fabrication of gas sensors, as a cathode material for solid state fuel cells, membranes for selective oxygen separation from gas mixtures etc. [4–6].

The physicochemical properties of $Sr_2FeMoO_{6-\delta}$ depend to a large extent on its oxygen stoichiometry which affects the superstructure ordering degree of iron and molybdenum cations, charge and spin degrees of freedom and hence the electron exchange between $Fe^{3+}$ and $Mo^{5+}$ [7–10]. The lattice distortions caused by the presence of defects in the anion sublattice affect the bond lengths and the spatial position of the $Fe^{3+}$—$O^{2}$—$Mo^{5+}$ chains by changing the exchange interaction integral which is controlled by the overlap of the electron orbits and the angle of the bond between them [11–13]. The presence of oxygen ions or their vacancies on the surface of the $Sr_2FeMoO_{6-\delta}$ grains favors the change of the electron

charge density at the grain boundaries and in the surface regions of the grains [14–16]. In this case the charge density is controlled by the partial oxygen pressure in the ambient gaseous media within the oxygen desorption temperature range and hence affects the electron transport properties of the compound thus allowing strontium ferromolybdate to be used as a resistive gas sensor. In this case the performance of the double perovskite device depends largely on the concentration and mobility of oxygen defects. The oxidation and reduction processes in the material may reversibly change the oxygen stoichiometry both in the grains and at the grain boundaries and hence the magnetic and galvanomagnetic properties of the double perovskite [17–19]. Therefore obtaining strontium ferromolybdate with reproducible physical properties, correct understanding of the processes occurring in the material and predicting the service life of the devices on its basis require a study of specimens with controlled oxygen content.

It should be noted that the homogeneity range of strontium ferromolybdate by the oxygen index is quite narrow, from $\delta = 0$ to $\delta = 0.086$. For example, annealing at 1473 K requires partial oxygen pressures within $\log p(O_2) = -10.20$ or lower $\log p(O_2) = -13.70$ because double perovskite will decompose in both cases. If the oxygen partial pressure exceeds the upper limit ($\log p(O_2) \geq -10.20$), then $Sr_2FeMoO_{6-\delta}$ decomposes according to the equation $Sr_2FeMoO_6 + 1/2O_2 = SrMoO_4 + SrFeO_3$, whereas below the limit $\log p(O_2) = -13.70$ it decomposes into simpler oxides followed by the formation of SrO, Fe and Mo [20]. Low partial oxygen pressures and the narrow allowable range $-13.70 \leq \log p(O_2) \leq -10.20$ makes the synthesis of the single phase compound with the required oxygen index a difficult task. Taking into account the above line of reasoning and the large effect of the intra-grain and grain surface oxygen on the physical properties of $Sr_2FeMoO_{6-\delta}$, one can conclude on the importance of information on the exchange processes between the complex oxide and the gaseous media. Thus, studying oxygen desorption is essential and important for the practical application of the abovementioned materials.

The aim of this work is to study oxygen desorption in $Sr_2FeMoO_{6-\delta}$ and to assess the energy of the anion mobility in the material as a function of structural defect concentration.

## 2. Experimental

The polycrystalline $Sr_2FeMoO_{6-\delta}$ specimens were synthesized from $SrFeO_{3-x}$ and $SrMoO_4$ precursors which were obtained using the standard ceramic technology from $MoO_3$ and $Fe_2O_3$ oxides and high grade strontium carbonate $SrCO_3$. Stoichometric mixtures of the raw reactants $SrCO_3 + 0.5Fe_2O_3$ and $SrCO_3 + MoO_3$ were ground in a vibration mill with spirit for 3 h. The processed mixtures were dried at 350 K and pressed into tablets. The $SrFeO_{3-x}$ and $SrMoO_4$ precursors were synthesized with preliminary anneals at 970 and 1070 °C for 20 and 40 h, respectively. To increase the homogeneity of the as-annealed mixtures we used additional grinding. The single phase $SrFeO_{3-x}$ compound was finally synthesized at $T = 1470$ K for 20 h in an argon gas flow, and the $SrMoO_4$ compound, at $T = 1470$ K for 40 h at $p(O_2) = 0.21 \cdot 10^5$ Pa followed by room temperature quenching. The oxygen content in the $SrFeO_{3-x}$ specimens was determined by weighing the specimens before and after complete reduction to simple SrO oxide and to metallic Fe in a hydrogen gas flow at 1470 K for 20 h. The initial specimens proved to have the composition $SrFeO_{2.52}$. The $SrFeO_{2.52} + SrMoO_4$ reactant mixtures pressed into 10 mm diameter 4–5 mm thick tablets were annealed in a $5\%H_2$/Ar gas flow at 1420 K for 5 h followed by room temperature quenching. The as-synthesized $Sr_2FeMoO_{6-\delta}$ tablets were single-phase. The oxygen content in the specimens was determined by weighing the specimens before and after complete reduction to simple SrO oxide and to metallic Fe and Mo in a hydrogen gas flow at 1570 K for 20 h. The initial specimens proved to have $\delta = 0.01$.

Oxygen desorption in strontium ferromolybdate was studied using a Setaram Labsys TG-DSC16 measuring instrument at different heating rates in the 300–1420 K range in a continuous $5\%H_2$/Ar gas flow. The specimens were exposed to the above treatment until reaching the thermodynamic equilibrium with the gas environment and then cooled to room temperature in the same gas flow. The achievement of the thermodynamic equilibrium was judged from the absence of specimen weight loss at a constant temperature. The specimens were weighed accurate to $\pm 3 \cdot 10^{-5}$ g.

The lattice parameters and the superstructure ordering degree of the cations ($P$) were determined using the Ritweld method with the ICSD-PDF2 (Release 2000) database and the POWDERCELL [21] and FullProf [22] software on the basis of X-ray diffraction data obtained using a DRON-3 instrument in Cu$K_\alpha$ radiation. The diffraction patterns were taken at room temperature at a 60 deg/h rate in the $\theta = 10$–$90$ deg range.

## 3. Results and Discussion

Oxygen desorption in $Sr_2FeMoO_{6-\delta}$ was studied using thermal gravimetric analysis at different heating rates ($v_h = 3$, 5, 7, 9 and 11 deg/min) in a continuous $5\%H_2$/Ar gas flow in the 300–1420 K range (Fig. 1).

Analysis of the oxygen desorption *vs* temperature curves showed that at any heating rate the oxygen index of the compound does not achieve saturation at $T = 1420$ K and depends on heating rate. At a 3 deg/min heating rate, intense oxygen desorption onsets at $T \sim 713$ K. Increasing the heating rate to 11 deg/min shifts the oxygen desorption onset to higher temperatures, i.e. ~775 K, Thus, increasing the heating rate affects oxygen desorption. This led to a tangible change in the $\Delta\delta = |\delta_{300K} - \delta_{1420K}|$ parameter which was $\Delta\delta = 0.088$ for $v_h = 3$ deg/min and

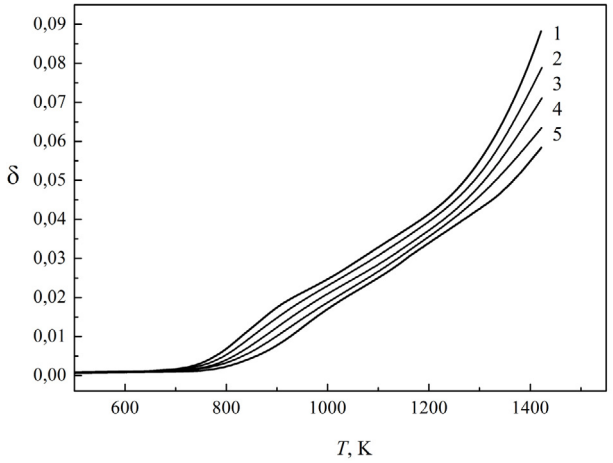


**Figure 1.** Oxygen nonstoichiometry degree *vs* temperature in $Sr_2FeMoO_{5.99}$ specimens for different heating rates: (1) 3, (2) 5, (3) 7, (4) 9 and (5) 11 deg/min

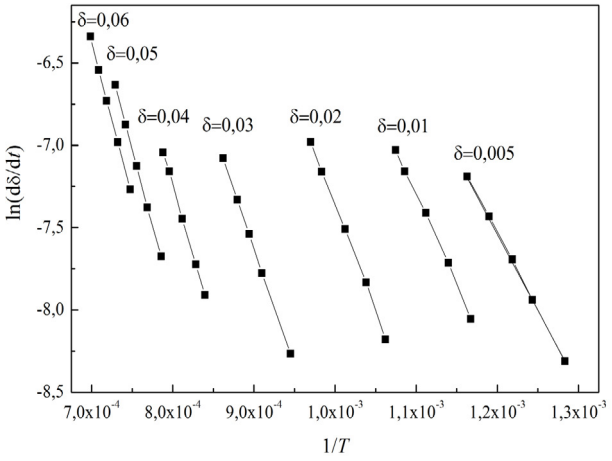


**Figure 2.** Change rate of $\ln(d\delta/dt)_v = f(1/T)$ for different oxygen indices

$\Delta\delta = 0.058$ for $v_h = 11$ deg/min, indicating that oxygen desorption depends on the concentration of anion defects in the $Sr_2FeMoO_{6-\delta}$ structure. The oxygen diffusion activation energy was calculated using the Merzhanov method [23]. The experimental $\delta = f(T)$ curves were used to determine the temperatures at which the oxygen nonstoichiometry was the same for different heating rates. Then the $\ln(d\delta/dt)_v$ - $f(1/T)$ functions were drawn for the chosen set of temperatures at constant δ (Fig. 2).

The tilt of the $\ln(d\delta/dt)_v = f(1/T)$ lines decreases monotonically with an increase in δ, indicating that the oxygen diffusion activation energy depends on the concentration of oxygen vacancies. The complex dependence of the oxygen mobility energy on the concentration of the anion defects in strontium ferromolybdate is confirmed by oxygen diffusion activation energy calculations ($E_a$) using the Merzhanov method according to the following formula:

$$E_a = -R\left\{\frac{d\ln\left(\frac{d\delta}{dt}\right)_v}{d\left(\frac{1}{T}\right)}\right\},$$

where $t$ is the process duration, $R$ is the universal gas constant and $T$ is the experiment temperature [23, 24]. At an early stage of oxygen desorption from $Sr_2FeMoO_{6-\delta}$ the oxygen diffusion activation energy is the lowest, i.e. ~76.7 kJ/mole at $\delta = 0.005$, and with an increase in the concentration of oxygen vacancies it increases and achieves saturation at $E_a = 156.3$ kJ/mole and $\delta = 0.06$ (Fig. 3).

To analyze the dependence of oxygen desorption from $Sr_2FeMoO_{6-\delta}$ on the process temperature and the δ parameter we graphically differentiated the $\delta = f(t, T)$ curves in order to trace the course of the $(d\delta/dt) = f(T)$ and $(d\delta/dt) = f(\delta)$ functions (Fig. 4). Analysis of these functions proved them to be non-homothetic at heating rates $v_h = 3$, 5, 7, 9 and 11 deg/min and $T = 300$–1420 K, indicating a change of the oxygen diffusion mechanism during the reduction of strontium ferromolybdate in the experimental temperature range.

We found the $d\delta/dt = f(T)$ and $d\delta/dt = f(\delta)$ functions to have a typical break which allows one to divide oxygen desorption in two process stages. The first stage (I) occurring in the $700 \le T \le 1100$ K range features a peak of the $d\delta/dt = f(T)$ function the absolute value of which shifts towards higher temperatures with an increase in $v_h$ due to the low mobility of the oxygen vacancies. The $d\delta/dt = f(\delta)$ function has the peak of oxygen desorption at the first stage (I) in a narrow range $0.012 < \delta < 0.014$ during $E_a$ growth, indicating that one of the oxygen desorption mechanisms can become predominant.

We now consider different oxygen positions in the $Sr_2FeMoO_{6-\delta}$ compound. The first and the most highly reactive variant is oxygen adsorbed by grain surface. Therefore at the first process stage the well-developed surface of the polycrystalline specimens makes the oxygen desorption rate in the ~700–1070 K range dependent on the reaction kinetics at the gas/solid interface. The growth of $E_a$ suggests oxygen desorption has a contribution of O1

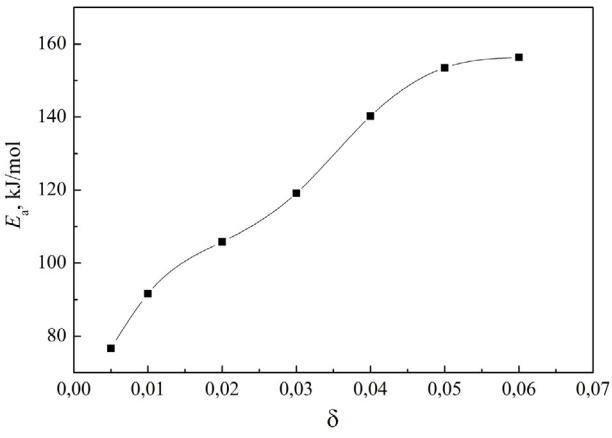


**Figure 3.** Oxygen diffusion activation energy $E_a$ *vs* oxygen nonstoichiometry degree

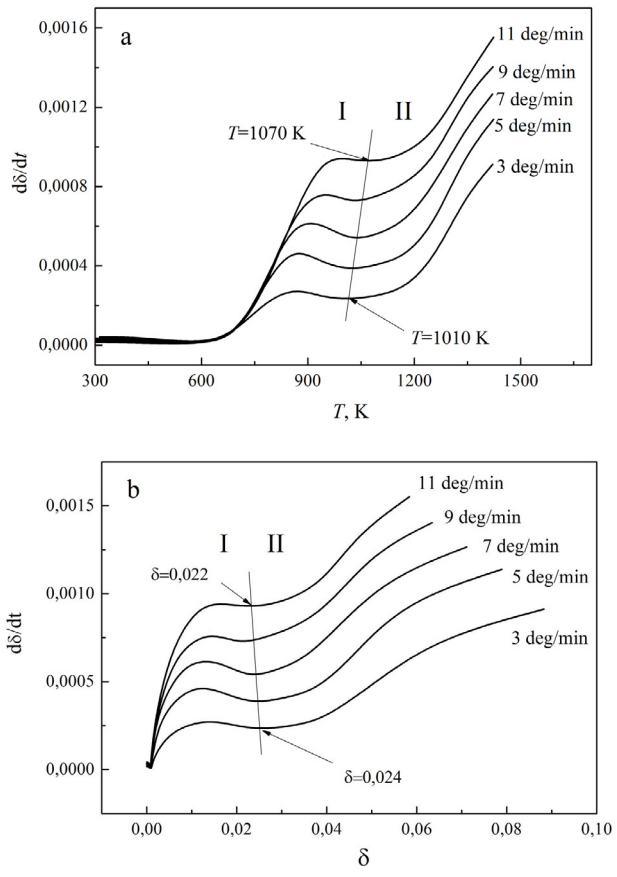


**Figure 4.** Oxygen desorption rate $Sr_2FeMoO_{6-\delta}$ vs different rate (*a*) heating temperature and (*b*) oxygen indices

and O2 anions having different crystallographic positions but almost similar bond energies.

Further increase in $T$ and δ (stage II) only causes an increase in $d\delta/dt$ without saturation. It is safe to assume that the second stage at $\delta \geq 0.024$ involves a change in the defect formation mechanism which affects the mobility of the anions. Quite possibly, an increase in the concentration of oxygen vacancies $V_o^{\bullet\bullet}$ causes their mutual interaction followed by ordering in the Fe/Mo-01 crystallographic planes with the formation of various types of associations. Similar observations were made by other researchers [20]. They proved that if the $V_o^{\bullet\bullet}$ point defects do not interact, the change in the oxygen nonstoichiometry $\delta = [V_o^{\bullet\bullet}]$ should have the following dependence on the partial oxygen pressure: $\delta = [V_o^{\bullet\bullet}] \sim p(O_2)^{-0.5}$, but this does not agree with the experimental results of the abovementioned authors. Since the experimental exponent of $p(O_2)^{-0.35}$ differs significantly from the expected one $n = -0.5$, one can conclude that the hypothesized formation mechanism of discrete oxygen vacancies is not authentic. Thus, the results of this experiment and earlier work [20] suggest that an increase in the concentration of oxygen vacancies to above $\delta \geq 0.024$ leads to their association which affects the defect formation mechanism, the mobility of the anions and hence the exponent of the partial oxygen pressure.

# 4. Summary

We showed that during oxygen desorption from $Sr_2FeMoO_{6-\delta}$ in polythermal mode at different heating rates the oxygen index depends on the heating rate and does not achieve saturation until $T$ = 1420 K. Oxygen diffusion activation energy calculation using the Merzhanov method showed that at an early stage of oxygen desorption from the $Sr_2FeMoO_{6-\delta}$ compound the oxygen diffusion activation energy is the lowest, ~ 76.7 kJ/mole at $\delta = 0.005$, and with an increase in the concentration of oxygen vacancies the oxygen diffusion activation energy grows to $E_a$ = 156.3 kJ/mole at $\delta = 0.06$. We found that the $d\delta/dt = f(T)$ and $d\delta/dt = f(\delta)$ functions have a typical break which allows one to divide oxygen desorption in two process stages. It is hypothesized that an increase in the concentration of oxygen vacancies $V_o^{\bullet\bullet}$ leads to their mutual interaction followed by ordering in the Fe/Mo-01 crystallographic planes with the formation of various types of associations.

# Acknowledgments

The support of the work in frames of the Deutsche Forschungsgemeinschaft (DFG) project no. SE 2714/2-1 and the European project H2020-MSCA-RISE-2017-778308-SPINMULTIFILM is gratefully acknowledged.

# References

1. Serrate D., De Teresa J.M., Ibarra M.R. Double perovskites with ferromagnetism above room temperature. *J. Phys.: Condensed Matter*. 2007; 19(2): 1–86. https://doi.org/10.1088/0953-8984/19/2/023201
2. Topwal D., Sarma D.D., Kato H., Tokura Y., Avignon M. Structural and magnetic properties of $Sr_2Fe_{1+x}Mo_{1-x}O_6$($-1 \leq x \leq 0.25$). *Phys. Rev. B.* 2006; 73(9): 0944191–0944195. https://doi.org/10.1103/PhysRevB.73.094419
3. Chana T.S., Liua R.S., Hub S.F., Linc J.G. Structure and physical properties of double perovskite compounds $Sr_2FeMO_6$ ($M$ = Mo, W). *Mater. Chem. Phys*. 2005;93(2–3):314–19. https://doi.org/10.1016/j.matchemphys.2005.03.060
4. Kovalev L.V., Yarmolich M.V., Petrova M.L., Ustarroz J., Terryn H.A., Kalanda N.A., Zheludkevich M.L. Double perovskite $Sr_2FeMoO_6$ films prepared by electrophoretic deposition. *ACC Appl. Mater. Interfaces*. 2014; 6(21): 19201–19206. https://doi.org/10.1021/am5052125
5. dos Santos-Gómez L., León-Reina L., Porras-Vázquez J.M., Losilla E.R., Marrero-López D. Chemical stability and compatibility of dou-

ble perovskite anode materials for SOFCs. *Solid State Ionics*. 2013; 239: 1–7. https://doi.org/10.1016/j.ssi.2013.03.005

6. Kalanda N., Kim D.-H., Demyanov S., Yu S.-C., Yarmolich M., Petrov A., Suhk K.O. $Sr_2FeMoO_6$ nanosized compound with dielectric sheaths for magnetically sensitive spintronic devices. *Current Appl. Phys*. 2018; 18(1): 27–33. https://doi.org/10.1016/j.cap.2017.10.018
7. Stoeffler D., Colis S. Oxygen vacancies or/and antisite imperfections in $Sr_2FeMoO_6$ double perovskites: an ab initio investigation. *J. Phys.: Condensed Matter*. 2005; 17(41): 6415–6424. https://doi.org/10.1088/0953-8984/17/41/012
8. Yarmolich M.V., Kalanda N.A., Yaremchenko A.A., Gavrilov S.A., Dronov A.A., Silibin M.V. Sequence of phase transformations and inhomogeneous magnetic state in nanosized $Sr_2FeMoO_{6-\delta}$. *Inorganic Materials*. 2017; 53(1): 96–102. https://doi.org/10.1134/S0020168517010186
9. Rager J., Zipperle M., Sharma A., MacManus-Driscoll J.L. Oxygen stoichiometry in $Sr_2FeMoO_6$, the determination of Fe and Mo valence states, and the chemical phase diagram of $SrO–Fe_3O_4–MoO_3$. *J. Am. Ceram. Soc*. 2004; 87(7): 1330–1335. https://doi.org/10.1111/j.1151-2916.2004.tb07730.x
10. Liscio F., Bardelli F., Meneghini C., Mobilio S., Ray S., Sarma D.D. Local structure and magneto-transport in $Sr_2FeMoO_6$ oxides. *Nuclear Instruments and Methods in Physics Research Section B: Beam Interactions with Materials and Atoms*. 2006; 246(1): 189–193. https://doi.org/10.1016/j.nimb.2005.12.033
11. Allub R., Navarro O., Avignon M., Alascio B. Effect of disorder on the electronic structure of the double perovskite $Sr_2FeMoO_6$. *Phys. B: Condensed Matter*. 2002;320(1–4):13–17. https://doi.org/10.1016/S0921-4526(02)00608-7
12. Tovar M., Causa M.T., Butera A., Navarro J., Martínez B., Fontcuberta J., Passeggi M.C.G. Evidence of strong antiferromagnetic coupling between localized and itinerant electrons in ferromagnetic $Sr_2FeMoO_6$. *Phys. Rev. B*. 2002; 66(2): 024409–1 (17p). https://doi.org/10.1103/PhysRevB.66.024409
13. Lindén J., Yamamoto T., Karppinen M., Yamauchi H. Evidence for valence fluctuation of Fe in $Sr_2FeMoO_{6-w}$ double perovskite. *Appl. Phys. Lett*. 2000; 76(20): 2925–2927. https://doi.org/10.1063/1.126518
14. Sarma D.D., Mahadevan P., Saha-Dasgupta T., Ray S., Kumar A. Electronic Structure of $Sr_2FeMoO_6$. *Phys. Rev. Lett.* 2000; 85(12): 2549–2552. https://doi.org/10.1103/PhysRevLett.85.2549
15. Niebieskikwiat D., Caneiro A., Sánchez R.D., Fontcuberta J. Oxygen-induced grain boundary effects on magnetotransport properties of $Sr_2FeMoO_{6-\delta}$. *Phys. Rev. B*. 2001; 64(18): 180406–1–4. https://doi.org/10.1103/PhysRevB.64.180406
16. Jurca B., Berthon J., Dragoe N., Berthet P. Influence of successive sintering treatments on high ordered $Sr_2FeMoO_6$ double perovskite properties. *J. Alloys and Compounds*. 2009;474(1–2):416–423. https://doi.org/10.1016/j.jallcom.2008.06.100
17. MacManus-Driscoll J., Sharma A., Bugoslavsky Y., Branford W., Cohen L.F., Wei M., Reversible low-field magnetoresistance in $Sr_2Fe_{2-x}Mo_xO_{6-\delta}$ by oxygen cycling and the role of excess Mo ($x > 1$) in grain-boundary regions. *Advanced Materials*. 2006; 18(7): 900–904. https://doi.org/10.1002/adma.200501277
18. Matsuda Y., Karppinen M., Yamazaki Y., Yamauchi H. Oxygen-vacancy concentration in $A_2MgMoO_{6-\delta}$ double-perovskite oxides. *J. Solid State Chemistry*. 2009; 182(7): 1713–1716. https://doi.org/10.1016/j.jssc.2009.04.016
19. Sharma A., MacManus-Driscoll J.L., Branford W., Bugoslavsky Y., Cohen L.F., Rager J. Phase stability and optimum oxygenation conditions for $Sr_2FeMoO_6$ formation. *Appl. Phys. Lett*. 2005; 87(11): 112505–1–3. https://doi.org/10.1063/1.2048810
20. Kircheisen R., Töpfer J. Nonstoichiometry, point defects and magnetic properties in $Sr_2FeMoO_{6-\delta}$ double perovskites. *J. Solid State Chemistry*. 2012; 185: 76–81. https://doi.org/10.1016/j.jssc.2011.10.043
21. Kraus W., Nolze G. POWDER CELL-a program for the representation and manipulation of crystal structures and calculation of the resulting X-ray powder patterns. *J. Appl. Cryst*. 1996; (3)29: 301–303. https://doi.org/10.1107/S0021889895014920
22. Rodríguez-Carvajal J. Recent developments of the program FULLPROF. Commission on powder diffraction (IUCr). Newsletter, 2001, vol. 26, pp. 12–19.
23. Merzhanov A.G., Barzykin V.V., Shteinberg A.S., Gontkovskaya V.T. Methodological Principles in studying chemical reaction kinetics under conditions of programmed heating. *Thermochimica Acta*. 1977; (3)21: 301–332. https://doi.org/10.1016/0040-6031(77)85001-6
24. Sánchez-Rodríguez D., Eloussifi H., Farjas J., Roura P., Dammak M. Thermal gradients in thermal analysis experiments: Criterions to prevent inaccuracies when determining sample temperature and kinetic parameters. *Thermochimica Acta*. 2014; 589: 37–46. https://doi.org/10.1016/j.tca.2014.05.001